CLK1 reorganizes the splicing factor U1-70K for early spliceosomal protein assembly

Brandon E. Aubol[a], Jacob M. Wozniak[a,b,c], Laurent Fattet[a], David J. Gonzalez[a,b,c], and Joseph A. Adams[a,1]

[a]Department of Pharmacology, University of California San Diego, La Jolla, CA 92093; [b]Skaggs School of Pharmacy and Pharmaceutical Sciences, University of California San Diego, La Jolla, CA 92093; and [c]Collaborative Center for Multiplexing Proteomics, University of California San Diego, La Jolla, CA 92093

Edited by Adrian R. Krainer, Cold Spring Harbor Laboratory, Cold Spring Harbor, NY, and approved February 11, 2021 (received for review August 28, 2020)

Early spliceosome assembly requires phosphorylation of U1-70K, a constituent of the U1 small nuclear ribonucleoprotein (snRNP), but it is unclear which sites are phosphorylated, and by what enzyme, and how such modification regulates function. By profiling the proteome, we found that the Cdc2-like kinase 1 (CLK1) phosphorylates Ser-226 in the C terminus of U1-70K. This releases U1-70K from subnuclear granules facilitating interaction with U1 snRNP and the serine-arginine (SR) protein SRSF1, critical steps in establishing the 5′ splice site. CLK1 breaks contacts between the C terminus and the RNA recognition motif (RRM) in U1-70K releasing the RRM to bind SRSF1. This reorganization also permits stable interactions between U1-70K and several proteins associated with U1 snRNP. Nuclear induction of the SR protein kinase 1 (SRPK1) facilitates CLK1 dissociation from U1-70K, recycling the kinase for catalysis. These studies demonstrate that CLK1 plays a vital, signal-dependent role in early spliceosomal protein assembly by contouring U1-70K for protein–protein multitasking.

kinase | phosphorylation | regulation | splicing

The splicing of precursor messenger RNA (pre-mRNA) occurs at the spliceosome, a multimegadalton complex composed of 5 small nuclear ribonucleoproteins (U1-6 snRNP) and over 100 proteins (1, 2). The assembly of this catalytic machine is a multistep process involving the exchange of numerous RNA-protein components leading to the active spliceosome. The first assembly stage involves U1 snRNP association at the 5′ splice site in pre-mRNA, an event guided by essential splicing factors known as the serine-arginine (SR) proteins, named for a C-terminal domain rich in arginine-serine (RS) dipeptides (3, 4). SR proteins contain one or two N-terminal RNA recognition motifs (RRMs) that bind exonic splicing enhancer (ESE) sequences near pre-mRNA splice sites (5). The RRMs are also important for U1 snRNP association at splice sites. An RRM (RRM1) from the SR protein SRSF1 (also known as ASF/SF2) binds the RRM from U1-70K, an essential protein substituent of U1 snRNP (6). Since U1 snRNP recognizes an intronic sequence from −2 to +6 along the 5′ splice site that includes only two conserved bases (GU), physical coupling of U1-70K to the SR protein that binds ESEs (five to seven nucleotides) provides additional specificity for proper 5′ splice-site assignment (7, 8). Importantly, these protein–protein assembly events are tightly regulated through SR protein phosphorylation. RS domain phosphorylation severs internal RS–RRM contacts within SRSF1, freeing its RRMs for both pre-mRNA binding and association with phosphorylated U1-70K in the U1 snRNP (6, 9, 10). While these posttranslational modifications are important for protein assembly, SR protein dephosphorylation is also required for attaining the fully active, mature spliceosome (11–13).

Much is known about how phosphorylation regulates the structure and function of SR proteins. SR protein kinase 1 (SRPK1) phosphorylates Arg-Ser dipeptides in the RS domain of SRSF1 generating a "hypo-phosphorylated" state that allows SR-specific transportin TRN-SR2 binding and nuclear localization (14–16). This modified state of SRSF1 includes mostly phosphorylation of Arg-Ser dipeptides toward the N terminus of the RS domain, a region referred to as RS1 (residues 204 to 224). In the nucleus, SRSF1 largely resides in nonmembrane compartments known as speckles (17). The Cdc2-like kinase 1 (CLK1) phosphorylates three additional sites (Ser-Pro dipeptides) in the SRSF1 RS domain generating a "hyper-phosphorylated" state that enhances SRSF1 diffusion from speckles where it then binds pre-mRNA initiating early spliceosome assembly (18, 19). Nuclear CLK1 releases autoinhibitory contacts within SRSF1 allowing association of an RRM (RRM1) with the RRM in U1-70K (6). NMR studies showed that CLK1 phosphorylation breaks contacts between the RS domain and several residues in RRM1 liberating RRM1 (9). Unlike SRPK1 that contains a conserved docking groove in its kinase domain, CLK1 relies upon a lengthy, disordered N terminus that recognizes the disordered RS domains in SR proteins (20, 21). This generates high-affinity substrate recognition but does not efficiently release the phospho-SR protein. Epidermal growth factor (EGF) stimulation solves this dilemma by increasing nuclear SRPK1 where it binds the N terminus of CLK1, releasing phospho-SR proteins from CLK1 (22). SRPK1–CLK1 complex formation also promotes efficient CLK1-specific phosphorylation of Ser-Pro dipeptides and diffusion of SR proteins from speckles for splicing (22, 23). Thus, CLK1 recruits SRPK1 for enhanced phosphorylation and kinase recycling.

Although U1-70K binding requires a phosphorylated SR protein (24, 25), U1-70K must also undergo phosphorylation to accept SR proteins. Previous complementation studies using U1 snRNP-depleted nuclear extracts and purified U1 snRNP incubated with either ATP or ATP-γS have shown that U1-70K phosphorylation supports spliceosome assembly and splicing activity whereas phosphatase-resistant thiophosphorylation allows assembly but not

Significance

Proteome size is greatly enhanced through alternative mRNA splicing, a process catalyzed by the macromolecular spliceosome. The initial step in spliceosome assembly involves the binding of U1 snRNP to the 5′ splice site in mRNA. SR proteins ensure the fidelity of this step by simultaneously binding to mRNA and U1-70K, a protein component of U1 snRNP. Although phosphorylation of U1-70K is required for coupling to the SR protein, the enzyme that catalyzes this modification and the activating mechanisms are unknown. Here, we show that the protein kinase CLK1 phosphorylates a specific serine in the splicing factor U1-70K, reorganizing its structure and relieving a repressor contact for integration into U1 snRNP and stable binding to the SR protein.

Author contributions: J.A.A. designed research; B.E.A., J.M.W., and L.F. performed research; B.E.A., J.M.W., and D.J.G. analyzed data; and J.A.A. wrote the paper.

The authors declare no competing interest.

This article is a PNAS Direct Submission.

Published under the PNAS license.

[1]To whom correspondence may be addressed. Email: j2adams@health.ucsd.edu.

This article contains supporting information online at https://www.pnas.org/lookup/suppl/doi:10.1073/pnas.2018251118/-/DCSupplemental.

Published April 2, 2021.

splicing (26). Such findings suggest that, similar to SR proteins, U1-70K must be phosphorylated early for spliceosome assembly and then dephosphorylated later for catalytic function. However, it is not clear which sites are modified, and by what protein kinase, and how such phosphorylation regulates U1-70K structure. SRPK1 has been shown to copurify with U1 snRNP and thus could serve this function, but it also binds CLK1 in the nucleus raising the question of whether it acts alone or in a kinase–kinase complex (22, 23, 27). To evaluate a possible role for CLK1, we used a combination of affinity-purification and phosphoproteomic approaches to identify CLK1 interactors and substrates. This dual-proteomic strategy pinpointed a CLK1-dependent phosphorylation site on U1-70K (Ser-226). We found that Ser-226 phosphorylation releases an internal contact between the C terminus and RRM in U1-70K. This structural change enhances U1-70K diffusion from subnuclear storage compartments, allows physical attachment of the U1-70K RRM to the RRMs in SRSF1, and promotes U1-70K binding to U1 snRNP-associated proteins. EGF stimulation induces nuclear SRPK1 translocation where it promotes CLK1 release from U1-70K, recycling the kinase for catalysis. These studies identify a prominent role for nuclear CLK1 in the assembly of vital protein complexes involved in early spliceosomal development.

Results

Proteomic Analyses of CLK1 Interactors and Phosphorylation Targets. To perform proteomic analyses for CLK1, we overexpressed a C-terminal, FLAG-tagged form of the kinase (CLK1-FLAG) (*SI Appendix*, Fig. S1*A*) and verified that it was localized to the nucleus of HeLa cells, similar to previous findings (28) (*SI Appendix*, Fig. S1*B*). To identify CLK1 interactors and substrates, we employed a dual, affinity-purification and phosphoproteomic analysis of CLK1 (Fig. 1*A*). CLK1-FLAG was purified from HeLa cell lysates in the absence of RNase treatment, and interacting proteins were quantified via multiplexed, quantitative proteomics (Dataset S1). In tandem, a phosphoproteomic screen was carried out using a time course of a CLK1 inhibitor, TG003, to identify potential CLK1 substrates (Dataset S2). The intersection of these experiments was used to pinpoint CLK1 interactors and possible direct substrates. As expected, CLK1 affinity purification primarily captured proteins involved in RNA binding/splicing (*SI Appendix*, Fig. S1*C*) including SRSF3/4 (*SI Appendix*, Fig. S1 *D* and *E*) as well as CLK1 itself (Fig. 1*B*). Six proteins demonstrated significant enrichment in the pull-down experiment as well as phosphorylation changes at one of the inhibited time points (Fig. 1*C*). Among these, U1-70K (encoded by the SNRPN70 gene) had the most significant *P* values across all experimental conditions (Fig. 1*D*) and the expected expression profile of a CLK1 interactor (Fig. 1*E*) and substrate (Fig. 1*F*), making it a prime candidate for further study. We also detected an additional, unique phosphopeptide containing the U1-70K p-S266 site, which demonstrated a similar trend in expression (*SI Appendix*, Fig. S1*F*), providing more support for these results.

CLK1 N Terminus Is Important for U1-70K Recognition. Having shown that CLK1 binds and induces U1-70K phosphorylation in our proteomic studies (Fig. 1), we next investigated how CLK1 interacts with this splicing factor. Since the intrinsically disordered CLK1 N terminus is essential for high-affinity SRSF1 binding (Fig. 2*A*), we speculated that it might be necessary for U1-70K recognition (21, 29). Indeed, we showed that CLK1-FLAG interacts with endogenous U1-70K in HeLa cell lysates whereas a construct lacking the N terminus (CLK1(ΔN)FLAG) does not (Fig. 2*B*). To confirm that the N terminus plays a role in binding CLK1 to U1-70K, we showed that a GST-tagged form purified from *Escherichia coli* (GST-N) associates with endogenous U1-70K in HeLa cell lysates (Fig. 2*C*). To isolate specific regions controlling this interaction, we divided the N terminus into three blocks of ∼50 residues. We found that block three removal (GST-N(Δ3)) had no measurable effect whereas removal of blocks two and three (GST-N(Δ23)) significantly decreased binding suggesting that block one alone is not sufficient for U1-70K binding (Fig. 2*C*). Exploring additional deletions, we found that GST-N(Δ13) and GST-N(Δ12) do not support stable interactions whereas GST-N(Δ1) bound well to U1-70K (Fig. 2*D*). These findings indicate that no single block facilitates binding alone and that a broader span controls U1-70K association, similar to prior observations regarding the CLK1 N terminus and the SRSF1 RS domain (28). To verify that CLK1 phosphorylates Ser-226, we purified from *E. coli* a GST-tagged protein fused to residues 203 to 245 from the U1-70K C terminus that contains this residue along with a second potential site (Ser-216) that we mutated to alanine (Fig. 2*E*). Although CLK1 readily phosphorylated GST-70K(SS) at one site, it did not phosphorylate GST-70K(SA) or GST-70K(AA), which remove one or both serines (Fig. 2*F*). Overall, these findings indicate that CLK1 broadly uses its disordered N terminus to recognize U1-70K and phosphorylate a specific serine in the C terminus.

CLK1 Controls U1-70K Binding to SRSF1 and U1 snRNP Proteins. Although prior in-vitro studies suggest that U1-70K phosphorylation promotes SRSF1 binding, an initiating step in spliceosome assembly, such studies did not establish which kinase is responsible in cells (26). To address whether CLK1 controls this event through Ser-226 phosphorylation, we down-regulated the kinase using small interfering RNA (siRNA) or chemical inhibition with TG003 and found impaired interaction of endogenous SRSF1 and U1-70K in HeLa cell lysates (Fig. 3*A*). Down-regulation also reduced interactions between U1-70K and one of the Sm proteins (SmB/B′) that constitute the heptameric ring along with several other proteins (U1A and U1C) associated with U1 snRNP (Fig. 3*A*) without affecting the binding of U1 small nuclear RNA (U1 snRNA) (Fig. 3*B*). These findings suggest that CLK1 regulates stable U1-70K binding with proteins associated with U1 snRNP. Prior studies showed that the survival motor neuron (SMN) protein complex both assembles the Sm cores of snRNP's and connects U1 snRNA, bound to U1-70K, for U1 snRNP biogenesis (30, 31). We found that CLK1 down-regulation weakens contacts between U1-70K and the SMN protein (Fig. 3*A*). To explore whether Ser-226 phosphorylation regulates these protein–protein contacts, we expressed U1-70K containing an N-terminal FLAG tag (FLAG-U1-70K) and showed that it interacts with endogenous SRSF1, SMN, and SmB/B′ in HeLa cell lysates whereas FLAG-U1-70K^{mut} containing an alanine mutation at Ser-226 does not (Fig. 3*C*). Also, TG003 blocked FLAG-U1-70K interactions with SRSF1, similar to endogenous U1-70K (Fig. 3*C*). In comparison, Ser-226 mutation did not impair U1-70K binding to U1 snRNA (Fig. 3*D*). Overall, these findings suggest that CLK1 phosphorylation connects U1-70K to an SR protein and several proteins associated with U1 snRNP.

Having shown that Ser-226 phosphorylation regulates U1-70K interactions with SRSF1, we next asked whether such phosphorylation couples the U1-70K:SRSF1 complex with mRNA. We showed previously that an RNA strand (AGGCGGAGGAAGC) containing an SRSF1-dependent ESE (underlined) binds with high affinity to recombinant SRSF1 (7, 29). We confirmed using a filter binding assay that this ^{32}P-labeled RNA interacted with SRSF1, an effect that was blocked by excess, unlabeled RNA (Trap), but did not interact well with a purified, His-tagged RRM derived from U1-70K (residues 92 to 202, His-RRM^{70K}) (Fig. 3*E*). These findings suggest that the ESE-containing RNA is specific for the RRMs in SRSF1 rather than the RRM in U1-70K. We next found that ^{32}P-labeled RNA interacted robustly with immunoprecipitated FLAG-U1-70K, an effect that was blocked by excess Trap (Fig. 3*F*). However, RNA association with FLAG-U1-70K^{mut} was significantly impaired, implying that phosphorylation regulates ESE binding (Fig. 3*F*). For these studies, we also confirmed that both FLAG-U1-70K and FLAG-U1-70K^{mut} were

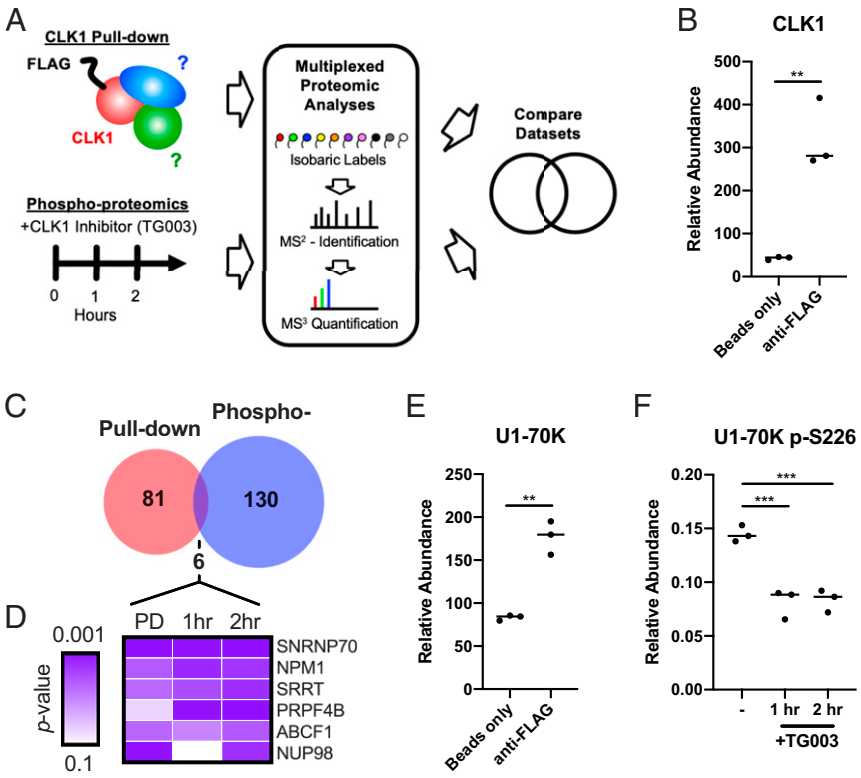

Fig. 1. Dual proteomic analysis identifies U1-70K as a CLK1 substrate. (*A*) Schematic of dual proteomic analysis. (*B*) CLK1 abundance from proteomic pull-down experiment. (*C*) Venn diagram for overlap of significant proteins from pull-down and phosphoproteomic experiment. (*D*) Heatmap of overlap-protein *P* values from various proteomic conditions. (*E*) U1-70K abundance from proteomic pull-down experiment. (*F*) U1-70K pS226 abundance after addition of TG003. Both pull-down and phosphoproteomic experiments were performed in triplicate ($n = 3$). For *B* and *E*, an unpaired Student's *t* test was used. For *F*, one-way ANOVA with Dunnett's multiple comparisons test was used. (ns, not significant; $^{**}P < 0.01$, $^{***}P < 0.001$.)

overexpressed at similar levels (Fig. 3*F*). Overall, these findings indicate that CLK1 phosphorylation of Ser-226 modifies U1-70K conformation, thereby allowing binding to SR proteins for enhanced recognition of ESE-containing mRNA.

CLK1 Regulates Intrasteric Connections in U1-70K. To explore the mechanism controlling CLK1-dependent binding of U1-70K to SRSF1, we investigated whether RNA serves as a bridge connecting endogenous SRSF1 and FLAG-U1-70K but found that RNase treatment of cell lysates did not impair interactions (Fig. 4*A*). Since prior studies showed that the bacterially expressed RRM from U1-70K interacts with RRM1 in SRSF1 (6), we speculated that the C terminus could regulate this intermolecular contact at the cellular level and in the context of the full-length protein. To evaluate which segment controls SRSF1 binding, we made deletions in FLAG-U1-70K^{mut} that removed two low-complexity regions (LC1 and LC2) previously identified (32) (Fig. 4*B*). We found that whereas removal of the C terminus fully restored SRSF1 binding, shorter deletions of either LC2 alone or LC1 and LC2 together did not (Fig. 4*B*). We also found that CLK1 binds to all constructs except FLAG-U1-70K(ΔC), implying that CLK1 binds residues 186 to 245 (Fig. 4*B*). We observed a decrease in CLK1 binding to one of the deletions outside this region, U1-70K^{mut}(Δ-LC2). This effect could reflect C-terminal conformational changes upon LC2 deletion that modifies CLK1 binding to residues 186 to 245. Furthermore, since LC1/2 deletion did not restore SRSF1 binding or abolish CLK1 binding, we conclude that the C-terminal GFP tag in FLAG-U1-70K^{mut} does not affect binding. A prior yeast two-hybrid study suggested that residues 248 to 270 in LC1 facilitate SRSF1 binding, but this study did not control for Ser-226 phosphorylation state, which we now show is the dominant driver for SRSF1 binding in the cell (33). Overall, these studies suggest that C-terminal residues connecting the RRM and LC1/2 (residues 186 to 245) are important for down-regulating SRSF1 binding to U1-70K.

To understand how the C terminus regulates U1-70K, we explored whether GST-70K(SS), which spans residues 203 to 245 and contains the Ser-226, interacts with the U1-70K RRM in a phosphorylation-dependent manner. We showed that the interaction of His-RRM^{70K} with GST-70K(SS) is disrupted by CLK1 phosphorylation (Fig. 4*C*). In comparison, CLK1 does not sever binding to the phosphorylation-resistant GST-70K(SA) suggesting that Ser-226 modification regulates these molecular contacts (Fig. 4*C*). We next wished to determine whether these contacts modulate SR protein binding. Since the unphosphorylated RS domain in SRSF1 interferes with RRM binding (9), we purified a GST-tagged SRSF1 lacking its regulatory RS domain (GST-SRSF1(ΔRS)) and showed that it binds to His-RRM^{70K} in the absence but not in the presence of GST-70K(SS) (Fig. 4*D*). These findings indicate that the CLK1 phosphorylatable peptide, derived from U1-70K, and the RRMs in SRSF1 compete for a common binding site on His-RRM^{70K}. In summary, our results suggest that CLK1 phosphorylation liberates repressive contacts between a polypeptide in the C terminus of U1-70K and its neighboring RRM, thereby permitting SR protein binding.

CLK1 Releases U1-70K from Nuclear Granules Affecting Splicing. U1-70K has been shown to localize in membrane-free, subnuclear structures such as speckles and Gemini of Cajal bodies (34–37). Since splicing occurs outside these nuclear granules on the speckle

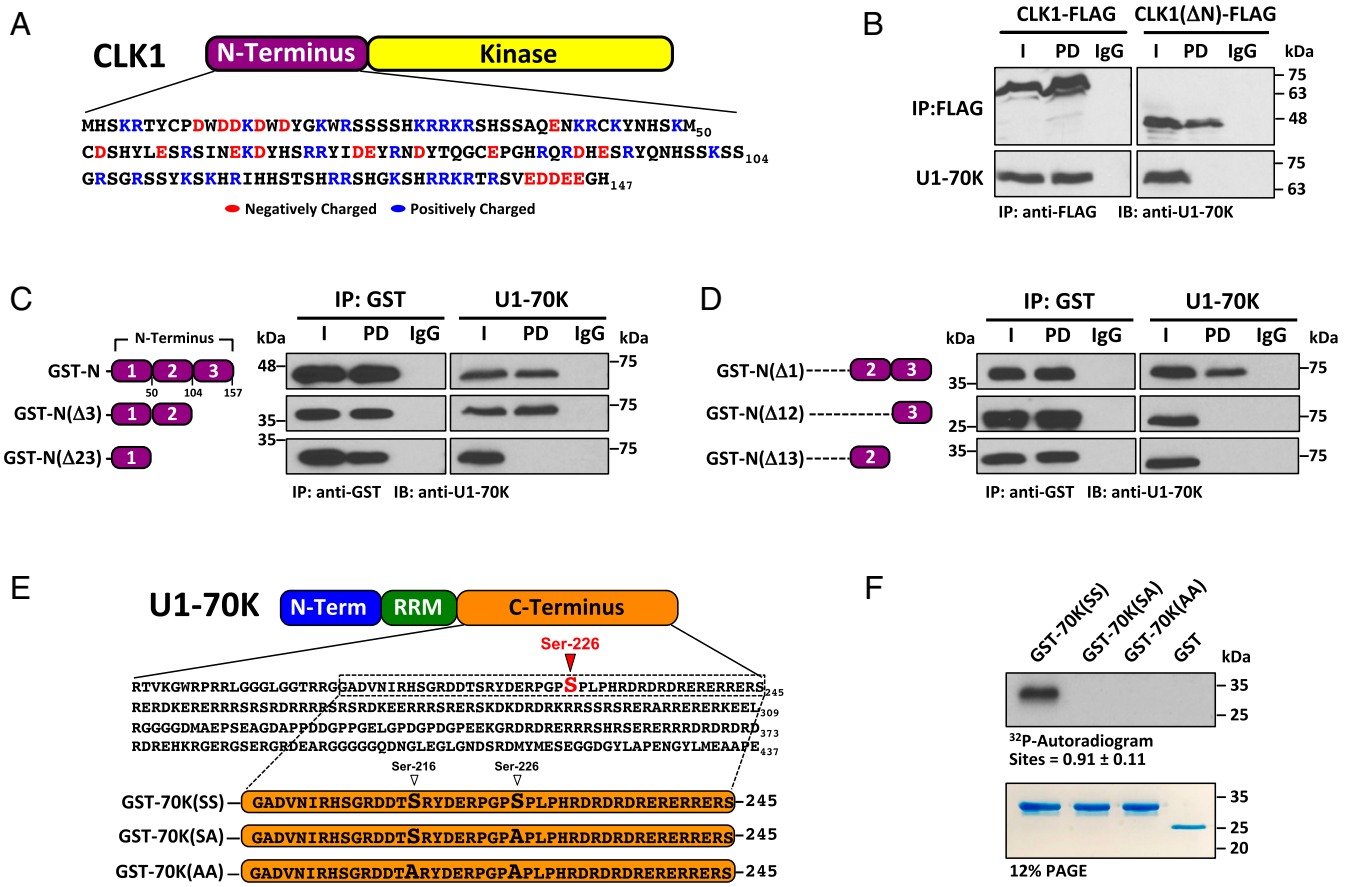

Fig. 2. CLK1 N Terminus controls U1-70K binding and phosphorylation. (*A*) Sequence of the CLK1 N terminus. (*B*) U1-70K binding depends on the CLK1 N terminus. CLK1-FLAG and CLK1(ΔN)-FLAG, expressed in HeLa cells, are immunoprecipitated using an agarose-conjugated anti-FLAG antibody. The displayed data reflect a representative of two separate experiments with similar results ($n = 2$). (*C* and *D*) U1-70K binding determinants are broadly distributed in the CLK1 N terminus. GST-N and several deletions, mixed with HeLa cell lysates, are immunoprecipitated using an agarose-conjugated anti-GST antibody. The IgG lanes in *B*–*D* represent the agarose resin controls lacking the conjugated antibody. (*E*) Sequence of the U1-70K C terminus and truncations attached to GST. (*F*) Phosphorylation of GST-70K(SS) and mutant forms from *E* using His-CLK1 and [^{32}P]ATP. The number of sites represents an average of three separate experiments ($n = 3$) along with SE.

periphery (38), we wondered whether CLK1 phosphorylation affects U1-70K subnuclear localization. We monitored the GFP tag in FLAG-U1-70K in HeLa cells and found that most fluorescence colocalized with SC35, a traditional marker for nuclear speckles and storage centers for U1 snRNP and SR proteins (Fig. 5*A*). CLK1-RFP expression induced diffusion of FLAG-U1-70K from granules to the nucleoplasm, a phenomenon blocked by TG003 (Fig. 5 *A* and *C*). To verify that this effect is due to Ser-226, the CLK1 phosphorylation site, we monitored FLAG-U1-70K^{mut} and found that CLK1-RFP overexpression had no effect on its subnuclear localization in the absence or presence of TG003 (Fig. 5 *B* and *C*). Such findings suggest that CLK1 phosphorylation of Ser-226 promotes U1-70K mobilization from nuclear granules. We next performed RT-PCR experiments to monitor the effects of Ser-226 on exon usage in three target genes—MYO1B, RBM10, and EIF5 (Fig. 5*D*). MYO1B has been shown to have two alternative exons whose inclusion is sensitive to SRSF1 expression owing to established SRSF1 binding sites in exons 23 and 24 (39). The alternative splicing of RBM10 and EIF5 can be induced by EGF stimulation and thus may be influenced by the SRPK1–CLK1 axis (40). We found that FLAG-U1-70K^{mut} enhanced exon exclusion for MYO1B and RBM10 compared to FLAG-U1-70K (Fig. 5*E*). FLAG-U1-70K(ΔC), lacking the repressive C terminus, exhibited effects similar to that of the wild-type splicing factor for two of the genes. In one case, FLAG-U1-70K^{mut} had no significant splicing effect compared to the wild-type protein although FLAG-U1-70K(ΔC) resulted in a small decrease in exon exclusion (EIF5). Such findings suggest that other factors outside the U1-70K C terminus may play a role in establishing certain alternative exons. Overall, these effects show that CLK1 phosphorylation of Ser-226 mobilizes U1-70K from subnuclear structures affecting exon usage.

SRPK1 Enhances CLK1 Phosphorylation and Dissociation from U1-70K. Although CLK1 phosphorylates SRSF1 for splicing function, it does not readily dissociate the phosphoproduct (22, 29). Since SRPK1 facilitates this dissociation through an SRPK1–CLK1 complex (22, 23), we explored whether SRPK1 could influence U1-70K release. We showed that, while SRPK1 does not phosphorylate GST-70K(SS), it enhances CLK1 activity toward this substrate by threefold (Fig. 6 *A* and *B*). In steady-state kinetic assays, we found that SRPK1 increases both the k_{cat} and k_{cat}/K_m for the peptide by three to fourfold (Fig. 6*C*). These findings suggest that SRPK1 is unlikely to phosphorylate Ser-226 but can up-regulate its phosphorylation through contacts with CLK1.

We next evaluated whether SRPK1 promotes U1-70K dissociation from CLK1 similar to SRSF1. We added a recombinant, kinase-inactive SRPK1 (kdSRPK1) to HeLa cell lysates and found that it dissociated endogenous CLK1 from the U1-70K:SRSF1 complex (Fig. 6*D*). Here, we used an inactive SRPK1 to avoid potential phosphorylation of other sites that may impact CLK1 binding. In our assays in Fig. 4*C*, we found that phosphorylation

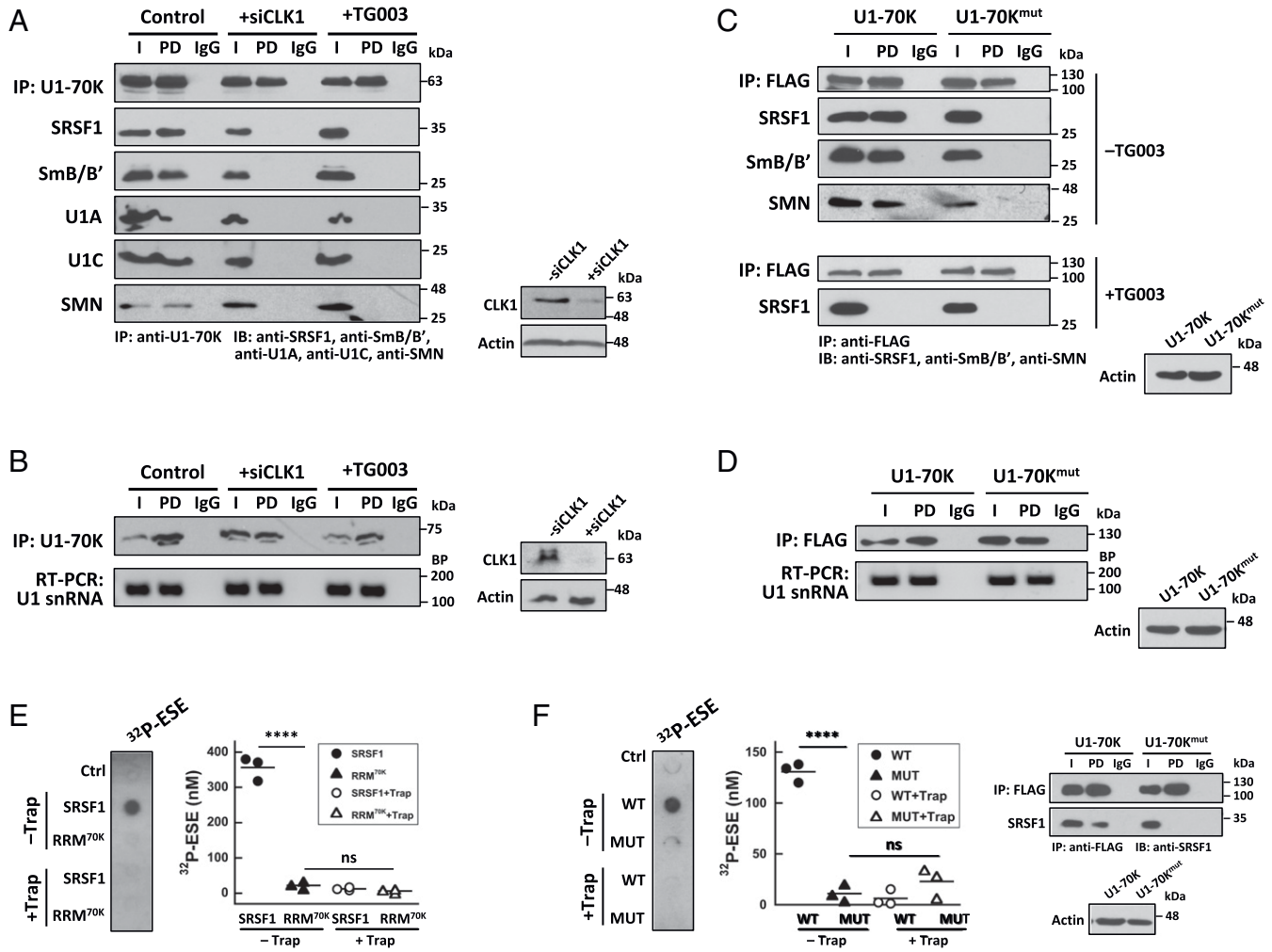

Fig. 3. CLK1 regulates U1-70K binding to SRSF1 and several U1 snRNP-related proteins. (*A* and *B*) CLK1 down-regulation impairs U1-70K interactions with SRSF1, SmB/B′, U1A, U1C, and SMN (*A*) but has no effect on U1 snRNA binding (*B*). HeLa cells are treated with siRNA for CLK1 or TG003, and U1-70K is immunoprecipitated from lysates using an agarose-conjugated anti–U1-70K antibody. U1 snRNA is detected using RT-PCR. Control refers to untreated cells. CLK1 knockdown efficiency is shown in matched lysates. The data in *A* and *B* reflect representatives of two separate experiments with similar results ($n = 2$). (*C* and *D*) Alanine replacement of Ser-226 in U1-70K impairs interactions with SRSF1, SmB/B′, and SMN (*C*) but has no effect on U1 snRNA binding (*D*). FLAG-U1-70K and FLAG-U1-70K^{mut} are immunoprecipitated from HeLa cell lysates using an agarose-conjugated anti-FLAG antibody. U1 snRNA is detected using RT-PCR. The displayed data reflect representatives of two separate experiments with similar results ($n = 2$). (*E*) RRM of U1-70K does not bind to an SRSF1-dependent ESE. SRSF1 and His-RRM^{70K}, incubated with a ^{32}P-labeled ESE (AGGCGGAGGAAGC) in the absence and presence of an unlabeled ESE (Trap), is absorbed onto a nitrocellulose membrane, washed, and counted. Ctrl refers to control samples lacking proteins. The dot plot shows the amount of ^{32}P bound to the membrane in three separate experiments ($n = 3$). (*F*) Alanine replacement of Ser-226 in U1-70K impairs interactions with an SRSF1-dependent ESE. FLAG-U1-70K and FLAG-U1-70K^{mut}, incubated with a ^{32}P-labeled ESE in the absence and presence of an unlabeled ESE (Trap), are immunoprecipitated from HeLa cell lysates using an agarose-conjugated anti-FLAG antibody, absorbed onto a nitrocellulose membrane, washed, and counted. Ctrl refers to control samples lacking cell lysates. The dot plot shows the amount of ^{32}P bound to the membrane in three separate experiments ($n = 3$). The expression levels of immunoprecipitated FLAG-tagged proteins and associated SRSF1 are confirmed by Western blotting. The IgG lanes in *A*–*D* and *F* represent the agarose resin controls lacking the conjugated antibody.

released CLK1 from the peptide substrate whereas such phosphorylation does not appear to be sufficient for CLK1 release from the full-length U1-70K (Fig. 6*D*). These findings suggest that whereas CLK1 largely contacts residues 203 to 245 within GST-70K(SS), sequences outside this minimal consensus region may either directly or indirectly further support high-affinity binding. To assess whether such a dissociative mechanism occurs naturally, we stimulated HeLa cells with EGF to induce increased nuclear SRPK1 and found enhanced CLK1 release from U1-70K:SRSF1 in nuclear extracts unless TG003 was added (Fig. 6*E*). We also observed SRPK1 and CLK1 binding to U1-70K without EGF suggesting that, in addition to CLK1 association with the C terminus, some SRPK1 may bind to other regions in U1-70K. Indeed, we showed that whereas the C terminus is required for CLK1 binding, it is dispensable for SRPK1 association suggesting that SRPK1 likely interacts with N-terminal sequences in U1-70K (*SI Appendix*, Fig. S2). We suspect that EGF stimulation increases nuclear SRPK1 above basal levels, thereby driving increased complex formation for CLK1 release. Overall, these studies suggest that, similar to SR proteins, SRPK1 up-regulates U1-70K release from CLK1, recycling the kinase for catalysis.

Discussion

Spliceosome initiation involves the phosphorylation-dependent interaction between an SR protein and U1-70K at the 5′ splice site in pre-mRNA (3, 4), but the regulatory mechanisms controlling this process are not fully understood. On the one hand, CLK1 activates the SR protein SRSF1 by severing a contact

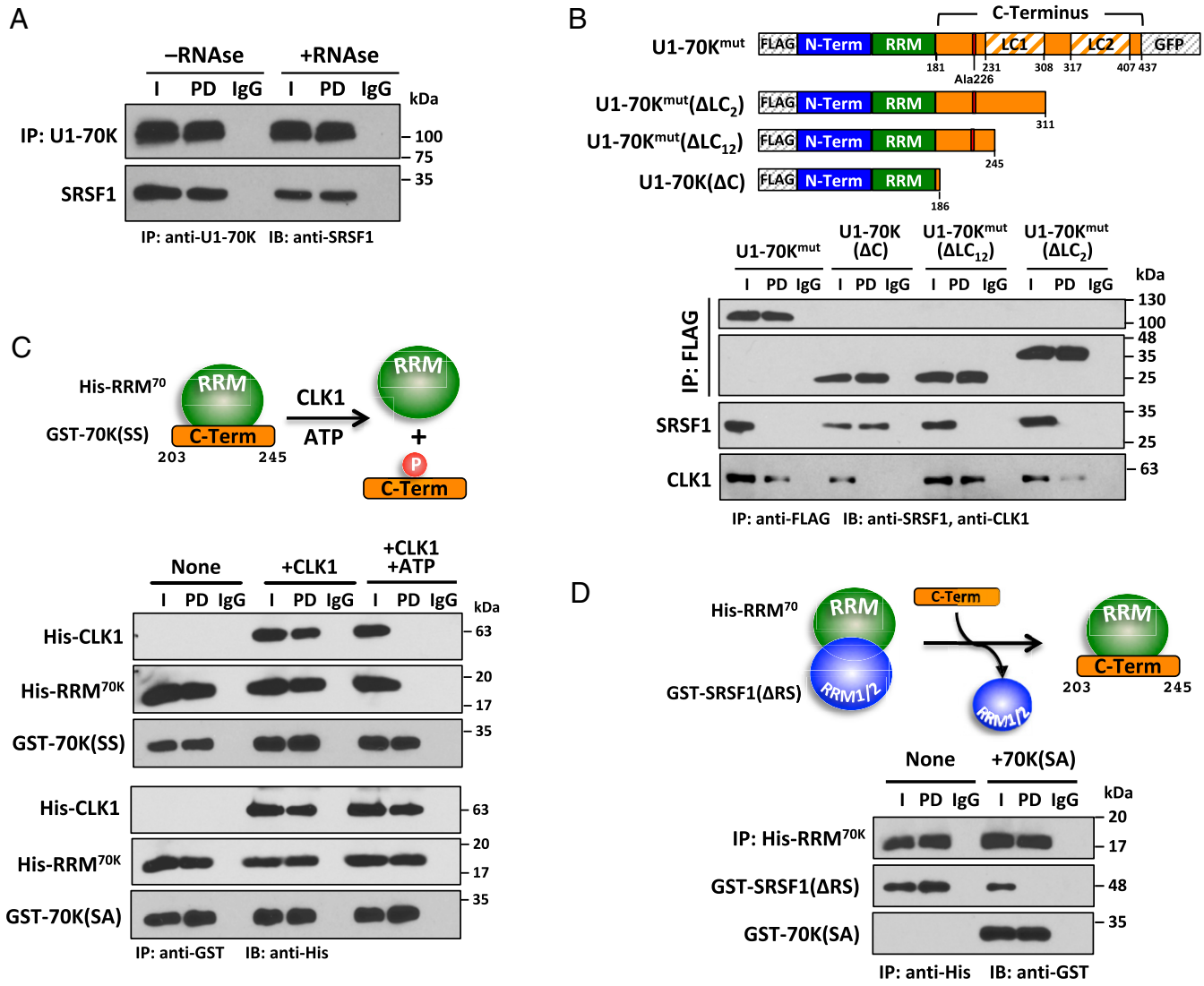

Fig. 4. Phosphorylation-dependent interactions between the C terminus and RRM^{70K} control U1-70K binding to SRSF1. (*A*) Effects of RNase on the U1-70K:SRSF1 complex. U1-70K is immunoprecipitated from HeLa cell lysates using an agarose-conjugated anti–U1-70K antibody. The displayed data reflect a representative of two separate experiments with similar results ($n = 2$). (*B*) C-terminal deletion in U1-70K^{mut} promotes SRSF1 binding. FLAG-tagged constructs expressed in HeLa cells are immunoprecipitated from lysates using an agarose-conjugated anti-FLAG antibody. (*C*) Interactions between the C terminus and RRM in U1-70K are disrupted by CLK1 phosphorylation. GST-tagged C-terminal peptides, incubated with His-RRM^{70K} in the absence and presence of CLK1 and ATP, are immunoprecipitated using an agarose-conjugated anti-GST antibody. The displayed data reflect a representative of two separate experiments with similar results ($n = 2$). (*D*) SRSF1 and C terminus compete for a common binding site on the RRM in U1-70K. His-RRM^{70K}, incubated with GST-SRSF1(ΔRS) in the absence and presence of GST-70K(SS), is immunoprecipitated using an agarose-conjugated anti-His antibody. The displayed data reflect a representative of two separate experiments with similar results ($n = 2$). The IgG lanes in *A*–*D* represent the agarose resin controls lacking the conjugated antibody.

between the C-terminal RS domain and an RRM allowing stable interactions with U1-70K, an essential component of U1 snRNP (6, 9) (Fig. 7). However, to accept the activated SR protein, U1-70K must also undergo phosphorylation-dependent activation although the nature of this step was not defined until now (26). In our investigations, we show that CLK1 activates U1-70K by phosphorylating Ser_{226} in a region separating the RRM and the larger, disordered C terminus of U1-70K. The resulting conformational switch frees the RRM in U1-70K for association with the RRMs in SRSF1 (Fig. 7). This structural change is likely facilitated by electrostatic repulsion between phospho-Ser_{226} and the RRM, similar to that observed for the RRMs and the phospho-RS domain in SRSF1 (9, 10), but it is also possible that phosphorylation could alter cis-trans isomerization of the flanking proline inducing more complex changes. Interestingly, signals that upregulate nuclear SRPK1 (e.g., EGF) also promote CLK1 release from phosphorylated U1-70K, recycling the kinase for subsequent catalytic steps. This bears similarities to SRPK1-induced dissociation of CLK1 from SR proteins and suggests a general release mechanism for splicing factors that avoids a stable, unproductive CLK1-product complex (22). These findings provide a link between extracellular signals and protein assembly mechanisms in the early spliceosome.

In addition to U1-70K:SRSF1 complex formation, our findings indicate that CLK1 plays a potential role in U1-70K integration into the U1 snRNP (Fig. 7). Assembly of the U1 snRNP for spliceosome initiation is a complex, stepwise process carried out in different cellular compartments. U1 snRNA, initially transcribed in the nucleus, is exported to the cytoplasm where the SMN complex attaches seven Sm proteins forming the core of the U1 snRNP followed by the addition of other components including U1A and U1C and several processing steps (30, 31).

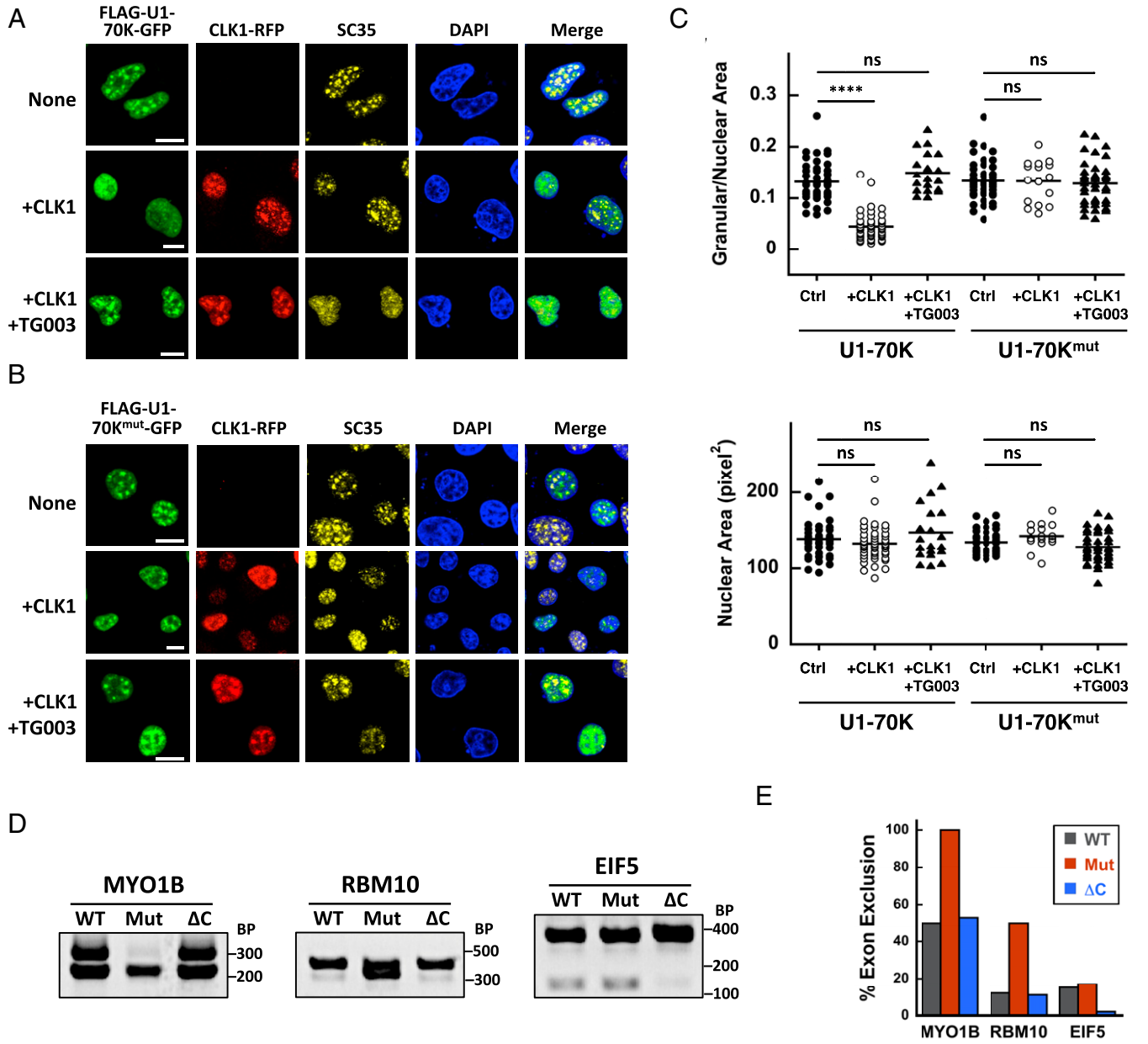

Fig. 5. CLK1 phosphorylation site controls U1-70K subnuclear localization and splicing. (*A* and *B*) Confocal imaging of FLAG-U1-70K (*A*) and FLAG-U1-70K^{mut} (*B*) with and without CLK1-RFP expression and TG003 in HeLa cells. Both U1-70K constructs and CLK1 are monitored by direct GFP and RFP fluorescence, and SC35 is monitored by immunofluorescence. None refers to cells expressing FLAG-U1-70K or FLAG-U1-70K^{mut} but no CLK1-RFP. (Scale bars, 10 μm.) (*C*) Granular and total nuclear areas for cells expressing FLAG-U1-70K and FLAG-U1-70K^{mut}. Areas are calculated from two separate transfection experiments ($n = 2$) using ImageJ. Results are displayed as dot plots where each dot represents an individual cell. *P* values are calculated using a one-way ANOVA test. ****$P < 0.0001$; $P > 0.05$ is designated as nonsignificant (ns). (*D*) Alternative splicing of several genes with U1-70K, U1-70K^{mut}, and U1-70K-ΔC expression. RT-PCR is performed on RNA samples from HeLa cells expressing FLAG-U1-70K (wild-type [WT]), FLAG-U1-70K^{mut} (mutant [Mut]), or FLAG-U1-70K(ΔC). The displayed data reflect a representative of two separate experiments with similar results ($n = 2$). (*E*) Bar graph shows the effects of U1-70K expression on splicing of genes from *C*. Percent exon exclusion is obtained from the average of two separate transfection experiments ($n = 2$) using ImageJ.

The ability of CLK1 to regulate U1-70K binding to both the SMN complex and several proteins associated with U1 snRNP in our investigations suggests that phosphorylation at Ser_{226} may induce a productive conformation for U1-70K attachment to U1 snRNP. Although our studies show that Ser-Pro phosphorylation induces structural changes for U1-70K integration, the potential role of the C terminus and its phosphorylation state within U1 snRNP is still not well understood. Crystallographic studies show that the U1-70K RRM interacts with stem loop 1 from U1 snRNA whereas the N terminus makes extensive contacts with U1C and the Sm ring (41) (Fig. 7). Although not present in the X-ray structure, the U1-70K C terminus may interact dynamically with U1C and SmB/B′ based on mass spectrometric studies of the native U1 snRNP (42). Further studies are needed to address the role of the C terminus within U1 snRNP and possible effects on splicing. Nonetheless, our findings show that CLK1 induces a phosphorylation-dependent conformational change in U1-70K that allows productive attachment to proteins associated with the U1 snRNP. These CLK1-induced structural changes can strengthen interactions between

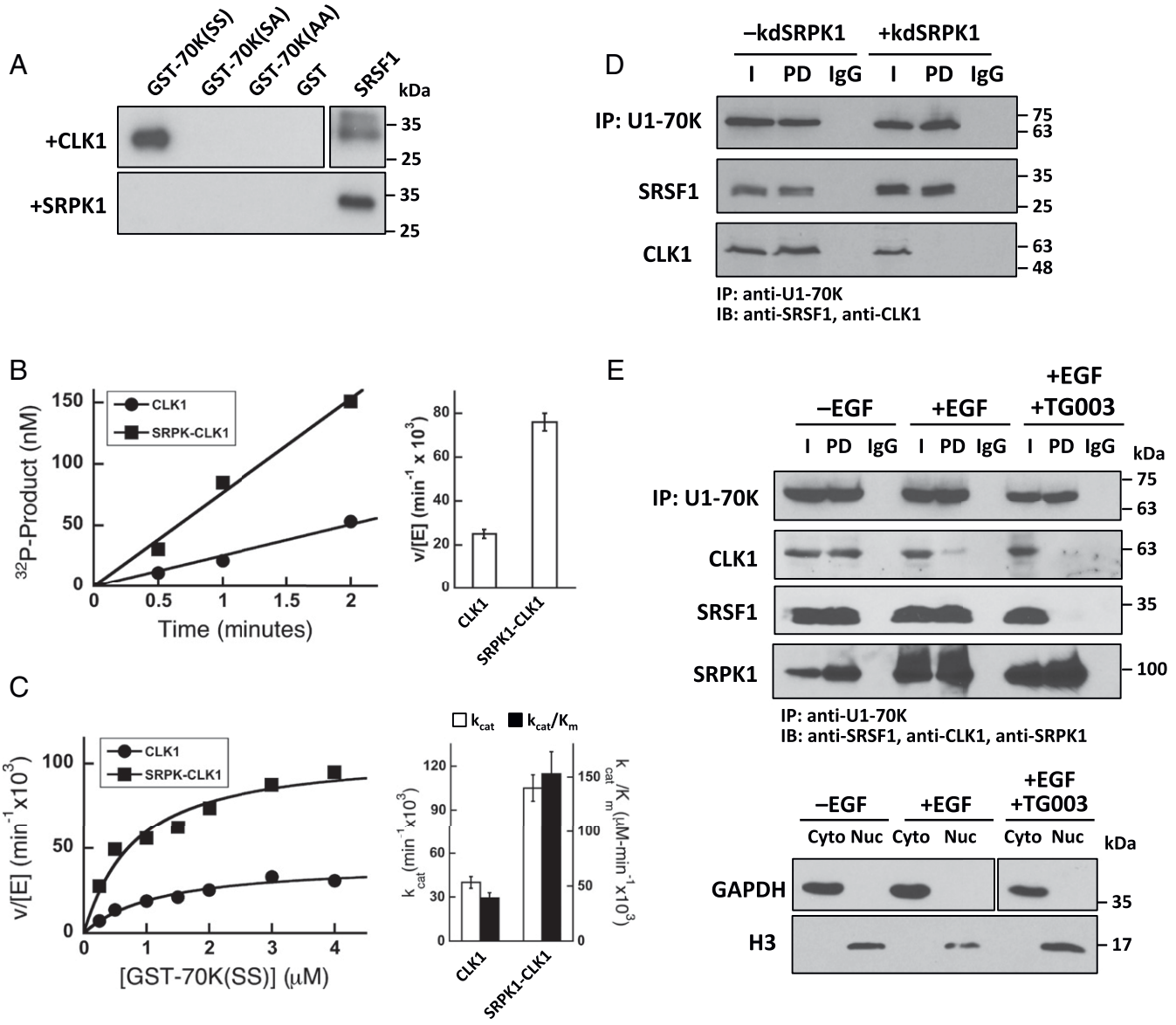

Fig. 6. SRPK1 promotes CLK1-dependent phosphorylation and dissociation of U1-70K. (*A*) SRPK1 does not phosphorylate the C-terminal peptide in U1-70K. GST-tagged C-terminal peptides and SRSF1 are incubated with [^{32}P]ATP and SRPK1 or CLK1 for 60 min. The displayed data reflect a representative of two separate experiments with similar results ($n = 2$). (*B*) CLK1 phosphorylation kinetics for GST-70K(SS) in the absence and presence of SRPK1. Each time course is the average of two separate experiments ($n = 2$). Initial velocities are shown in the bar graphs, and the error bars reflect SDs from the linear fits to the time courses. (*C*) Steady-state kinetic parameters for CLK1 with and without SRPK1. Enzyme-normalized initial velocities (v/[E]) are plotted as a function of total GST-70K(SS) and fitted to Eq. 1 to obtain k_{cat} and k_{cat}/K_m values presented in the bar graph. (*D*) SRPK1 promotes dissociation of CLK1 from U1-70K. Recombinant kdSRPK1 (1 μM) is added to HeLa cell lysates and endogenous U1-70K is immunoprecipitated using an agarose-conjugated anti–U1-70K antibody. (*E*) EGF promotes CLK1 dissociation from U1-70K. Endogenous U1-70K is immunoprecipitated from nuclear fractions of EGF-stimulated HeLa cells using an agarose-conjugated anti–U1-70K antibody. The IgG lanes in *C* and *D* represent the agarose resin controls lacking the conjugated antibody.

U1-70K and mRNA via enhanced bridging interactions with an SR protein.

Conclusions. The generation of multiple proteins from a single gene is essential for proteome expansion and complex biological functions. The spliceosome accomplishes this task through a large protein-RNA complex that recognizes splice sites near exon–intron boundaries, removes introns, and combines select exons in a regulated manner. Since early studies first established that the spliceosome requires protein factors such as SRSF1 and U1-70K that promote initiation, and that their function is strongly phosphorylation dependent, identifying the catalysts involved and their regulatory mechanisms is critical for understanding protein diversity. In this study, we found that the protein kinase CLK1 controls the first step in spliceosome assembly. CLK1 orchestrates protein–protein interactions between an SR protein and U1-70K by relieving repressive interactions in the latter (Fig. 7). CLK1 phosphorylation reorganizes the U1-70K architecture freeing its RRM for SR protein binding. This reorganization also provides the structural switch that allows U1-70K to interact with the SMN complex and the Sm ring system in U1 snRNP, thereby linking the SR protein to the critical initiator of the spliceosome. It is interesting that although SR proteins and U1-70K serve highly unique roles in the spliceosome, they are regulated by similar mechanisms.

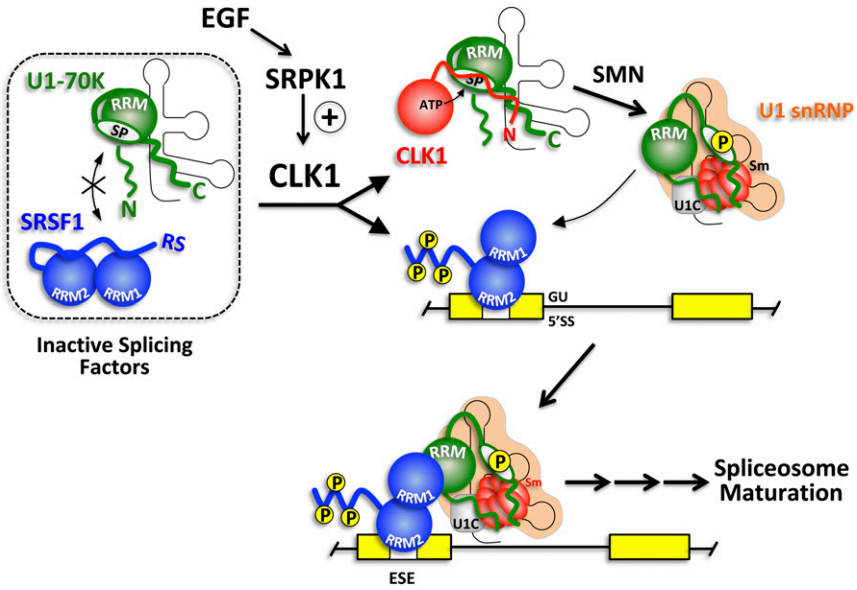

Fig. 7. Model showing how CLK1 binds and activates U1-70K for splicing function. CLK1 N terminus recognizes the C terminus of U1-70K allowing the kinase domain to phosphorylate Ser-226. Phosphorylation severs internal contacts allowing the RRM of U1-70K to bind the RRMs from SRSF1 and the C terminus of U1-70K to interact with U1 snRNP.

In both cases, a flexible C terminus rich in low-complexity residues blocks N-terminal, flanking RRMs from establishing protein–protein interactions (Fig. 7). The nuclear kinase CLK1 not only unleashes these RRMs for splice-site recognition but also is subject to regulation through an SRPK1–CLK1 axis connecting these phosphorylation events to external signals.

Methods

Materials. ATP, Mops, Hepes, Tris, $MgCl_2$, $MnCl_2$, NaCl, KCl, DTT, ethylenediaminetetraacetic acid (EDTA), Brij 35, Nonidet P-40, glycerol, acetic acid, lysozyme, DNase, RNase, Phenix imaging film, bovine serum albumin (BSA), Ni-resin, glutathione, and liquid scintillant were obtained from Fisher Scientific. [γ-^{32}P]ATP, FuGene and Lipofectamine 2000 were obtained from NEN Products, Promega, and ThermoFisher, respectively. Protease inhibitor mixture, EGF, and TG003 were obtained from Roche. Anti-GFP antibodies were obtained from Abcam. Anti-SmB/B′ antibodies, anti-CLK1/4 antibodies, agarose-conjugated anti-SNRNP70 antibodies, agarose-conjugated anti-GST antibodies, agarose-conjugated anti-GFP antibodies, and agarose-conjugated anti-His antibodies were obtained from Santa Cruz Biotechnology. Anti-Histone H3 antibodies, anti-FLAG antibodies, and agarose-conjugated anti-FLAG antibodies were purchased from Cell Signaling. Anti-GST antibodies, anti-Actin antibodies, anti-SNRNP70 antibodies, anti-SRPK1 antibodies, and anti-GAPDH antibodies were purchased from BioLegend, Sigma, Abcam, BD Transduction Laboratories, and Genscript, respectively. InstantBlue was purchased from Expedeon and CLK1 siRNA from Bioneer.

Expression and Purification of Recombinant Proteins. All forms of recombinant SRPK1 and SRSF1 were expressed and purified from pET19b vectors containing an N-terminal His tag as previously described (43). CLK1 virus was transfected and expressed in Hi5 insect cells, and CLK1 protein was purified with a nickel resin using a previously described procedure (20). CLK1-RFP was expressed from vector pcDNA3-mRFP. Bacterially expressed His-tagged RRM from U1-70K was expressed from a pET-15b vector. Mammalian FLAG-U1-70K constructs were expressed from pcDNA3.1(+)-C-eGFP vectors. All proteins containing a GST tag were expressed and purified from a pGEX6P-1 vector as previously described (29). All oligos were purchased from Integrated DNA Technologies. Hybond ECL nitrocellulose blotting membrane was from Amersham. Filter binding assays were performed using a Bio-Dot microfiltration apparatus from Bio-Rad. KinaseMax Kit was purchased from Ambion.

Immunoprecipitation and Knockdown Experiments. Immobilized bead conjugate (10 μL), mixed overnight at 4 °C with 200 μL HeLa cell lysates, was washed four times with 500 μL 1× phosphate-buffered saline (PBS) and centrifuged at 1,000 × *g*. Western immunoblotting was used to visualize protein bands. The Cell Signaling Fractionation Kit (no. 9038) was used to fractionate HeLa cells. Whole-cell lysates were prepared by treating cells with ice-cold 1× radioimmunoprecipitation assay (RIPA) buffer before sonication. For knockdown experiments, Lipofectamine 2000 was used to transfect 50 pmol siRNA in a 12-well poly-D-lysine plate. For inhibitor and growth factor addition experiments, growth media was supplemented with either 20 μM TG003 or 200 ng/mL EGF.

Confocal Imaging Experiments. To perform imaging experiments, cells were washed with 1× PBS and treated with 1% paraformaldehyde for 20 min at room temperature. Cells were then permeabilized at 4 °C for 10 min using PBS 0.5% Triton X-100 and blocked with 20% goat serum in PBS (blocking buffer). Cells were incubated overnight in blocking buffer containing primary antibody, washed three times with 1× PBS, incubated for 60 min with secondary antibodies at room temperature (goat anti-mouse AlexaFluor 647—Life), washed three times with 1× PBS, and then mounted in DAPI-containing mounting medium (Vector Laboratories). An Olympus FV1000 microscope with 405, 488, 555, and 647 laser lines was used to acquire cell images. These images were analyzed in a linear fashion with pseudocoloring using ImageJ software.

Phosphorylation Reactions. Phosphorylation progress curves were carried out using SRSF1 (1 μM) or U1-70K peptide constructs (1 μM) with SRPK1 (0.3 μM) or CLK1 (1 μM) in the presence of 100 mM Mops (pH 7.4) and 10 mM Mg^{2+} at 37 °C, using 50 μM [^{32}P]ATP with a specific activity of 4,000 to 8,000 cpm/pmol. For steady-state kinetic assays, CLK1 (200 nM) with or without SRPK1 (200 nM) is mixed with 25 μM [^{32}P]ATP and varying GST-70K(SS) (0.25 to 4 μM) in the presence of 100 mM Mops (pH 7.4) and 10 mM Mg^{2+} at 37 °C. All enzymatic reactions were conducted in 10 μL total volume and then quenched with the addition of 10 μL sodium dodecyl sulfate/polyacrylamide gel electrophoresis (SDS/PAGE) loading buffer. SDS-PAGE (14%) was used to separate phosphorylated SR proteins from unreacted [^{32}P]ATP. Phosphorylated SR proteins were cut from the dried gel and counted in liquid scintillant on the ^{32}P channel of the scintillation machine. The initial velocity versus substrate data were fit to Eq. 1:

$$\frac{v}{E_o} = k_{cat}\frac{S_o + E_o + K_m - \sqrt{(S_o + E_o + K_m)^2 - 4E_oS_o}}{2E_o}, \quad [1]$$

where v is the initial velocity, k_{cat} is the maximum rate constant, K_m is the Michaelis–Menten constant, and S_o and E_o are the total substrate and enzyme concentrations.

Splicing Assay and snRNA Detection. For splicing assays, the RNeasy Plus kit from Qiagen was used to isolate total RNA. The SuperScript III Reverse transcriptase from Invitrogen was then used to convert the isolated RNA to complementary DNAs (cDNAs). Select genes were then amplified using the GoTaq Green Master Mix (Promega) and oligo sets for these genes. The amplified fragments were resolved by 2% agarose gel and imaged by a Bio-Rad gel doc system. The following forward/reverse oligo sets were used for the denoted exons: MYO1B forward (exon 22): AGAGGTACCAGCAGACAAAGA; MYO1B reverse (exon 24): GATCCAAGCCAGTAAGCCCA; RBM10 forward (exon 3): GCAAGCATGACTATGACG ACTC; RBM10 reverse (exon 6): CTGAT TGGCTTCCATCCATCG; EIF5 forward (exon 1): CAGAGCGAGAACATTCCAGAG; and EIF5 reverse (exon 3): CAAGAGTTCTCGGTCTC TGAC. For snRNA amplification, RNA was isolated from immunoprecipitated lysates and amplified using oligos specific to U1 snRNA. U1-snRNA forward primer was GGCAGGGGAGATACCATGATCAC and U1-snRNA reverse primer was GCGCGAACGCAGTCCCCCACTACC.

RNA Binding Assay. Pull-down experiments were performed with a ^{32}P-labeled RNA oligomer based on an ESE from the RON oncogene (5′-AGGCGGAGGAAG C-3′). Labeling was carried out using the KinaseMax kit from Ambion and confirmed by 12% Urea PAGE. Immunoprecipitated lysates SRSF1 or RRM^{70K} were incubated with 1,000 nM ^{32}P-labeled ESE for 30 min at room temperature in 100 mM Mops (pH 7.2), 10 mM free Mg^{2+}, 5 mg/mL BSA, 75 mM NaCl, 10% glycerol, and 0.2 U/μL RNase inhibitor in a total volume of 50 μL. After incubation, samples were bound to a 0.45 μm nitrocellulose blotting membrane using a Bio-Rad Bio-Dot Apparatus and washed three times with 400 μL wash buffer (20 mM Tris, pH 7.5, and 100 mM NaCl). Filter spots for each sample were cut from the membrane and counted.

Cell Lysis and Protein Digestion. Following CLK1 immunoprecipitation or inhibition experiments described above, samples were prepared for mass spectrometry (MS)-based proteomic analysis. For phosphoproteomics, cells were lysed in a lysis buffer consisting of 1 mM phenylmethanesulfonyl fluoride, 1 mM β-glycerophosphate, 75 mM NaCl, 1 mM Na_3VO_4, 1 mM NaF, 10 mM $Na_4P_2O_7$, and 1× cOmplete, Mini, EDTA-free Protease Inhibitor in 50 mM Hepes, pH 8.5. Following cell lysis/immunoprecipitation, proteins were denatured via addition of an equal volume of 8 M Urea in 50 mM Hepes, pH 8.5 and then reduced and alkylated using dithiothreitol (30 min, 56 °C) and iodoacetamide (20 min, room temperature [RT] in the dark). Alkylated proteins were precipitated using chloroform and methanol for the phosphoproteomics and trichloroacetic acid for the immunoprecipitation experiments. Precipitated proteins were washed twice with ice-cold acetone, dried on a 56 °C heat block, then resuspended in digest buffer (1 M Urea, 50 mM Hepes, pH 8.5). Proteins were digested in a two-step process with LysC (16 h, RT) and trypsin (6 h, 37 °C). Digests were acidified by addition of trifluoracetic acid, then desalted using Seppaks. For phosphoproteomics, digested peptides were quantified using the Pierce Quantitative Colorimetric Peptide Assay and aliquoted for standard (50 μg) and phospho (2.5 mg)-proteomic runs. For immunoprecipitation experiments, all digested peptides were retained for subsequent analyses.

Phosphopeptide Enrichment. Phosphopeptides were enriched as previously described (44, 45). TiO2 beads were washed once with binding buffer (2 M lactic acid and 50% acetonitrile), once with elution buffer (50 mM KH_2PO_4, pH 10), then twice more with binding buffer. Desalted peptides were resuspended in binding buffer, mixed with beads at a ratio of 4:1 (beads to peptides) and vortexed for 1 h at RT. Beads were then washed with binding buffer (three times) followed by wash buffer (50% acetonitrile/0.1% trifluoracetic acid; three times). Phosphopeptides were eluted with two 5 min incubations in elution buffer while vortexing. Peptides were then desalted again with Seppaks, lyophilized, and stored at −80 °C until tandem mass tag (TMT) labeling.

TMT Labeling and Fractionation. Aliquoted peptides from each experiment were subject to TMT labeling. A pooled standard sample containing an equal amount of peptide from each sample was also included for data normalization. Samples were mixed in a random order and labeled with TMTs according to manufacturer instructions. Labeled samples were then mixed and desalted as above. Desalted samples were solubilized in 5% formic acid/5% acetonitrile and fractionated with a 4.6 mm × 250 mm C18 column using an Ultimate 3000 HPLC. The 96 acquired fractions were then combined into 24 fractions for regular proteomics (of which 12 alternating fractions were run) or 12 fractions for phosphoproteomics and dried prior to MS analysis.

LC-MS Analysis. Liquid chromatography-mass spectrometry (LC-MS) analysis was conducted on an Easy-nLC 1000 in line with an Orbitrap Fusion MS. Samples were resuspended in 5% formic acid/5% acetonitrile and separated on an in-house prepared column (inner diameter [I.D.] 100 μm, outer diameter [O.D.] 360 μm; ∼0.5 cm of 5 μm C_4 resin, ∼0.5 cm of 3 μm C_{18} resin and ∼29 cm of 1.8 μm C_{18} resin; 30 cm final length). Peptides were eluted from the column (heated to 60 °C) with a gradient of 11 to 30% acetonitrile in 0.125% formic acid (165 min) followed by a 100% acetonitrile wash (15 min) with 2,000 V applied through the T-junction used for electrospray ionization. MS instrument acquisition settings are previously described (44, 45).

Data Processing and Analysis. Proteome Discoverer 2.1 was used for processing raw MS files. The SEQUEST-HT algorithm was used to query MS2 spectra against the *Homo sapiens* Uniprot proteome (downloaded: May 2017, 59,010 entries). A decoy search against the reverse proteome was conducted to filter peptide and protein assignments to a false discovery rate (FDR) of <1% (46, 47). Tolerances of 50 ppm (MS1) and 0.6 Da (MS2) were used. Static modifications used in the search were TMT 10-plex labels (lysine and peptide *N*-termini) and carbamidomethylation (cysteines). Variable modifications used in the search were oxidation (methionine) and, for phosphoproteomics, phosphorylation (serine, threonine, and tyrosine). A fully tryptic digest was specified with up to two missed cleavages allowed. MS3 spectra were profiled for TMT reporter ions for multiplexed quantitation (48, 49). The signal-to-noise values of all peptides per protein were summed to obtain protein-level quantitation. Data were normalized as previously described (44, 50). Phosphosites were localized in the context of their full protein using the PTMphinder R package (51). Sample groups were compared using unpaired Student's *t* tests (pull-down data) and one-way ANOVA with Dunnett's multiple comparisons test (phosphoproteomic data). Gene-ontology analysis (52, 53) was performed to identify protein groups and pathways enriched in sets of proteins.

Data Availability. Proteomic data have been deposited in ProteomeXchange and MassIVE [accession nos. MSV000085972/PXD020978 (54) and MSV000085973/PXD020979 (55)].

ACKNOWLEDGMENTS. This work was supported by NIH Grants GM67969 and GM98528 to J.A.A., NIH Grants T32 GM007752 and T32 AR064194 to J.M.W., and NIH Grants R01AI148417 and R21AI149090 to D.J.G.

1. M. S. Jurica, M. J. Moore, Pre-mRNA splicing: Awash in a sea of proteins. *Mol. Cell* **12**, 5–14 (2003).
2. D. F. Stojdl, J. C. Bell, SR protein kinases: The splice of life. *Biochem. Cell Biol.* **77**, 293–298 (1999).
3. J. D. Kohtz *et al*., Protein-protein interactions and 5′-splice-site recognition in mammalian mRNA precursors. *Nature* **368**, 119–124 (1994).
4. J. Y. Wu, T. Maniatis, Specific interactions between proteins implicated in splice site selection and regulated alternative splicing. *Cell* **75**, 1061–1070 (1993).
5. J. C. Long, J. F. Caceres, The SR protein family of splicing factors: Master regulators of gene expression. *Biochem. J.* **417**, 15–27 (2009).
6. S. Cho *et al*., Interaction between the RNA binding domains of Ser-Arg splicing factor 1 and U1-70K snRNP protein determines early spliceosome assembly. *Proc. Natl. Acad. Sci. U.S.A.* **108**, 8233–8238 (2011).
7. H. X. Liu, M. Zhang, A. R. Krainer, Identification of functional exonic splicing enhancer motifs recognized by individual SR proteins. *Genes Dev.* **12**, 1998–2012 (1998).
8. H. X. Liu, S. L. Chew, L. Cartegni, M. Q. Zhang, A. R. Krainer, Exonic splicing enhancer motif recognized by human SC35 under splicing conditions. *Mol. Cell. Biol.* **20**, 1063–1071 (2000).
9. B. E. Aubol, P. Serrano, L. Fattet, K. Wüthrich, J. A. Adams, Molecular interactions connecting the function of the serine-arginine-rich protein SRSF1 to protein phosphatase 1. *J. Biol. Chem.* **293**, 16751–16760 (2018).
10. P. Serrano *et al*., Directional phosphorylation and nuclear transport of the splicing factor SRSF1 is regulated by an RNA recognition motif. *J. Mol. Biol.* **428**, 2430–2445 (2016).
11. J. E. Mermoud, P. T. Cohen, A. I. Lamond, Regulation of mammalian spliceosome assembly by a protein phosphorylation mechanism. *EMBO J.* **13**, 5679–5688 (1994).
12. J. E. Mermoud, P. Cohen, A. I. Lamond, Ser/Thr-specific protein phosphatases are required for both catalytic steps of pre-mRNA splicing. *Nucleic Acids Res.* **20**, 5263–5269 (1992).
13. Y. Shi, B. Reddy, J. L. Manley, PP1/PP2A phosphatases are required for the second step of Pre-mRNA splicing and target specific snRNP proteins. *Mol. Cell* **23**, 819–829 (2006).
14. A. Velazquez-Dones *et al*., Mass spectrometric and kinetic analysis of ASF/SF2 phosphorylation by SRPK1 and Clk/Sty. *J. Biol. Chem.* **280**, 41761–41768 (2005).
15. M. C. Lai, R. I. Lin, S. Y. Huang, C. W. Tsai, W. Y. Tarn, A human importin-beta family protein, transportin-SR2, interacts with the phosphorylated RS domain of SR proteins. *J. Biol. Chem.* **275**, 7950–7957 (2000).

16. M. C. Lai, R. I. Lin, W. Y. Tarn, Transportin-SR2 mediates nuclear import of phosphorylated SR proteins. *Proc. Natl. Acad. Sci. U.S.A.* **98**, 10154–10159 (2001).
17. D. L. Spector, Macromolecular domains within the cell nucleus. *Annu. Rev. Cell Biol.* **9**, 265–315 (1993).
18. M. M. Keshwani *et al*., Conserved proline-directed phosphorylation regulates SR protein conformation and splicing function. *Biochem. J.* **466**, 311–322 (2015).
19. B. E. Aubol *et al*., Partitioning RS domain phosphorylation in an SR protein through the CLK and SRPK protein kinases. *J. Mol. Biol.* **425**, 2894–2909 (2013).
20. M. M. Keshwani *et al*., Nuclear protein kinase CLK1 uses a non-traditional docking mechanism to select physiological substrates. *Biochem. J.* **472**, 329–338 (2015).
21. K. Colwill *et al*., The Clk/Sty protein kinase phosphorylates SR splicing factors and regulates their intranuclear distribution. *EMBO J.* **15**, 265–275 (1996).
22. B. E. Aubol *et al*., Release of SR proteins from CLK1 by SRPK1: A symbiotic kinase system for phosphorylation control of pre-mRNA splicing. *Mol. Cell* **63**, 218–228 (2016).
23. B. E. Aubol, M. M. Keshwani, L. Fattet, J. A. Adams, Mobilization of a splicing factor through a nuclear kinase-kinase complex. *Biochem. J.* **475**, 677–690 (2018).
24. S. H. Xiao, J. L. Manley, Phosphorylation of the ASF/SF2 RS domain affects both protein-protein and protein-RNA interactions and is necessary for splicing. *Genes Dev.* **11**, 334–344 (1997).
25. W. Cao, S. F. Jamison, M. A. Garcia-Blanco, Both phosphorylation and dephosphorylation of ASF/SF2 are required for pre-mRNA splicing in vitro. *RNA* **3**, 1456–1467 (1997).
26. J. Tazi *et al*., Thiophosphorylation of U1-70K protein inhibits pre-mRNA splicing. *Nature* **363**, 283–286 (1993).
27. R. Mathew *et al*., Phosphorylation of human PRP28 by SRPK2 is required for integration of the U4/U6-U5 tri-snRNP into the spliceosome. *Nat. Struct. Mol. Biol.* **15**, 435–443 (2008).
28. A. George, B. E. Aubol, L. Fattet, J. A. Adams, Disordered protein interactions for an ordered cellular transition: Cdc2-like kinase 1 is transported to the nucleus via its Ser-Arg protein substrate. *J. Biol. Chem.* **294**, 9631–9641 (2019).
29. B. E. Aubol *et al*., N-terminus of the protein kinase CLK1 induces SR protein hyperphosphorylation. *Biochem. J.* **462**, 143–152 (2014).
30. D. J. Battle *et al*., The SMN complex: An assembly machine for RNPs. *Cold Spring Harb. Symp. Quant. Biol.* **71**, 313–320 (2006).
31. B. R. So *et al*., A U1 snRNP-specific assembly pathway reveals the SMN complex as a versatile hub for RNP exchange. *Nat. Struct. Mol. Biol.* **23**, 225–230 (2016).
32. I. Bishof *et al*., RNA-binding proteins with basic-acidic dipeptide (BAD) domains self-assemble and aggregate in Alzheimer's disease. *J. Biol. Chem.* **293**, 11047–11066 (2018).
33. W. Cao, M. A. Garcia-Blanco, A serine/arginine-rich domain in the human U1 70k protein is necessary and sufficient for ASF/SF2 binding. *J. Biol. Chem.* **273**, 20629–20635 (1998).
34. N. Saitoh *et al*., Proteomic analysis of interchromatin granule clusters. *Mol. Biol. Cell* **15**, 3876–3890 (2004).
35. S. R. Kundinger, I. Bishof, E. B. Dammer, D. M. Duong, N. T. Seyfried, Middle-down proteomics reveals dense sites of methylation and phosphorylation in arginine-rich RNA-binding proteins. *J. Proteome Res.* **19**, 1574–1591 (2020).
36. A. Sharma, H. Takata, K. Shibahara, A. Bubulya, P. A. Bubulya, Son is essential for nuclear speckle organization and cell cycle progression. *Mol. Biol. Cell* **21**, 650–663 (2010).
37. E. Stejskalová, D. Staněk, The splicing factor U1-70K interacts with the SMN complex and is required for nuclear gem integrity. *J. Cell Sci.* **127**, 3909–3915 (2014).
38. P. Sacco-Bubulya, D. L. Spector, Disassembly of interchromatin granule clusters alters the coordination of transcription and pre-mRNA splicing. *J. Cell Biol.* **156**, 425–436 (2002).
39. X. Zhou *et al*., Splicing factor SRSF1 promotes gliomagenesis via oncogenic splice-switching of MYO1B. *J. Clin. Invest.* **129**, 676–693 (2019).
40. Z. Zhou *et al*., The Akt-SRPK-SR axis constitutes a major pathway in transducing EGF signaling to regulate alternative splicing in the nucleus. *Mol. Cell* **47**, 422–433 (2012).
41. Y. Kondo, C. Oubridge, A. M. van Roon, K. Nagai, Crystal structure of human U1 snRNP, a small nuclear ribonucleoprotein particle, reveals the mechanism of 5′ splice site recognition. *eLife* **4**, e04986 (2015).
42. H. Hernández *et al*., Isoforms of U1-70k control subunit dynamics in the human spliceosomal U1 snRNP. *PLoS One* **4**, e7202 (2009).
43. B. E. Aubol, J. A. Adams, Recruiting a silent partner for activation of the protein kinase SRPK1. *Biochemistry* **53**, 4625–4634 (2014).
44. J. M. Wozniak *et al*., Molecular dissection of Chagas induced cardiomyopathy reveals central disease associated and druggable signaling pathways. *PLoS Negl. Trop. Dis.* **14**, e0007980 (2020).
45. J. D. Lapek Jr, M. K. Lewinski, J. M. Wozniak, J. Guatelli, D. J. Gonzalez, Quantitative temporal viromics of an inducible HIV-1 model yields insight to global host targets and phospho-dynamics associated with vpr. *Mol. Cell Proteomics* **16**, 1447–1461 (2017).
46. J. E. Elias, W. Haas, B. K. Faherty, S. P. Gygi, Comparative evaluation of mass spectrometry platforms used in large-scale proteomics investigations. *Nat. Methods* **2**, 667–675 (2005).
47. J. E. Elias, S. P. Gygi, Target-decoy search strategy for increased confidence in large-scale protein identifications by mass spectrometry. *Nat. Methods* **4**, 207–214 (2007).
48. L. Ting, R. Rad, S. P. Gygi, W. Haas, MS3 eliminates ratio distortion in isobaric multiplexed quantitative proteomics. *Nat. Methods* **8**, 937–940 (2011).
49. G. C. McAlister *et al*., MultiNotch MS3 enables accurate, sensitive, and multiplexed detection of differential expression across cancer cell line proteomes. *Anal. Chem.* **86**, 7150–7158 (2014).
50. J. D. Lapek, Jr, M. K. Lewinski, J. M. Wozniak, J. Guatelli, D. J. Gonzalez, Quantitative temporal viromics of an inducible HIV-1 model yields insight to global host targets and phospho-dynamics associated with protein vpr. *Mol. Cell. Proteomics* **16**, 1447–1461 (2017).
51. J. M. Wozniak, D. J. Gonzalez, *PTMphinder*: An R package for PTM site localization and motif extraction from proteomic datasets. *PeerJ* **7**, e7046 (2019).
52. D. W. Huang *et al*., The DAVID gene functional classification tool: A novel biological module-centric algorithm to functionally analyze large gene lists. *Genome Biol.* **8**, R183 (2007).
53. W. Huang, B. T. Sherman, R. A. Lempicki, Systematic and integrative analysis of large gene lists using DAVID bioinformatics resources. *Nat. Protoc.* **4**, 44–57 (2009).
54. D. J. Gonzalez, CLK1 Pulldown Human Proteomic Interactors. ProteomeXchange and MassIVE. http://proteomecentral.proteomexchange.org/cgi/GetDataset?ID=PXD020978. Deposited 18 August 2020.
55. D. J. Gonzalez, CLK1 Inhibition Human Phosphoproteomics. ProteomeXchange and MassIVE. http://proteomecentral.proteomexchange.org/cgi/GetDataset?ID=PXD020979. Deposited 18 August 2020.